January 2017

Enhanced Optical Wireless Channel For Indoor And Intravehicle Communications: Power Distribution And Signal To Noise Ratio Analysis

Rana Rageh Shaaban

ENHANCED OPTICAL WIRELESS CHANNEL FOR INDOOR AND INTRAVEHICLE COMMUNICATIONS: POWER DISTRIBUTION AND SIGNAL TO NOISE RATIO ANALYSIS

by

Rana Rageh Shaaban
Bachelor of Science in Electronics & Telecommunication Engineering, Arab Academy for Science and Technology, 2013

A Thesis
Submitted to the Graduate Faculty
of the
University of North Dakota
in partial fulfillment of the requirements

for the degree of

Master of Science

Grand Forks, North Dakota
December
2017

This thesis, submitted by Rana Shaaban in partial fulfillment of the requirements for the Degree of Master of Science from the University of North Dakota, has been read by the Faculty Advisory Committee under whom the work has been done and is hereby approved.

12/05/17

Saleh Faruque

12/06/17

Prakash Ranganthan

12/6/2017

Naima Kaabouch

12/5/2017

William Semke

This thesis is being submitted by the appointed advisory committee as having met all of the requirements of the School of Graduate Studies at the University of North Dakota and is hereby approved.

Dean of the Graduate School

December 6, 2017

Date

PERMISSION

Title	Enhanced Optical Wireless Channel For Indoor and Intravehicle Communications: Power Distribution and Signal to Noise Ratio Analysis
Department	Electrical Engineering
Degree	Master of Science

In presenting this thesis in partial fulfillment of the requirements for a graduate degree from the University of North Dakota, I agree that the library of this University shall make it freely available for inspection. I further agree that permission for extensive copying for scholarly purposes may be granted by the professor who supervised my thesis work or, in his absence, by the chairperson of the department or the dean of the Graduate School. It is understood that any copying or publication or other use of this thesis or part thereof for financial gain shall not be allowed without my written permission. It is also understood that due recognition shall be given to me and to the University of North Dakota in any scholarly use which may be made of any material in my thesis.

Signature 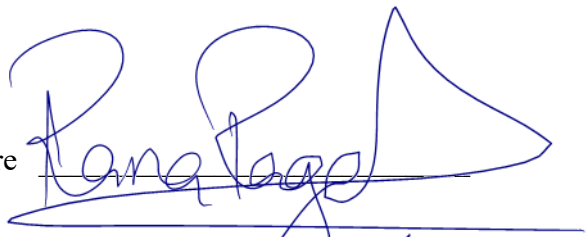

Date 12/06/2017

TABLE OF CONTENTS

LIST OF FIGURE

LIST OF TABLES

ACKNOWLEDGEMENTS

I would first like to thank my thesis advisor Prof. Saleh Faruque at the University of North Dakota. The door to Prof. Faruque office was always open whenever I ran into a trouble spot or had a question about my research or writing. He consistently allowed this paper to be my own work, but steered me in the right the direction whenever he thought I needed it.

I would also like to acknowledge Prof. William Semke, Prof. Naima Kaabouch, and Dr. Prakash Ranganathan at the University of North Dakota as the second readers of this thesis, and I am gratefully indebted to them for their very valuable comments on this thesis.

I would also like to thank the Electrical Engineering Department at the University of North Dakota for giving me this opportunity and financial support to finish my thesis.

Finally, I must express my very profound gratitude to my parents and to my spouse for providing me with unfailing support and continuous encouragement throughout my years of study and through the process of researching and writing this thesis. This accomplishment would not have been possible without them. Thank you.

To my family.

ABSTRACT

Visible light communication—(VLC) provides wide bandwidth and high security capabilities for free space optical communication. This thesis presents the key concepts, underlying principles and practical applications of visible light communications. In particular, this thesis focuses on the received power distribution pattern and signal to noise ratio for line-of-sight indoor and vehicular applications. Several methods are used to modify the SNR and power distribution levels. It is shown that in the absence of obstruction, the optical footprint is nearly circular and offers a platform for large- scale deployment in commercial environments, which is similar to micro and Pico cells.

By studying various kinds of commonly used VLC channel analysis: diffuse and line of sight channels, a simple improved indoor and intra-vehicular VLC transmission model for power distribution and SNR is presented. Employing optical wireless communications within the vehicle not only enhances user mobility, but also alleviates radio frequency interference, and lowers system cost through the utilization of license free spectrum. Moreover, a solution to increase the received power by changing the semi angle at half power is presented. The simulation results show the improved received power distribution and SNR. A VLC system, based on color-shift-keying (CSK) modulation and code-division multiple-access (CDMA) is presented. CSK–CDMA VLC system is used to enhance the VLC system capacity and mitigate single color light interference, which allows multiple users to access the network.

CHAPTER 1

INTRODUCTION

1.1 Literature Review

The Radio-frequency (RF) spectrum has been congested, since it is extensively used in wireless based communications systems. RF applications vary from short range indoor communications such as near field communications (NFC), Wi-Fi or Bluetooth to mobile cellular networks up to medium-to-long range links such as satellite-to Earth communications. Wireless communication plays an essential role in our daily live [1]. It is expected that future mobile data volume per area and number of connected devices will be increasing, respectively, higher than present wireless networks. To sustain such a high density and high capacity wireless communication is challenging.

One of the key candidates to solve the capacity crunch in certain applications is the visible light communications (VLC), which potentially offers 10,000 times more bandwidth capacity than the RF based technologies [2]. The VLC technology is mostly based around the intensity modulation of white light emitting diodes (LEDs), which can be switched on and off at a very high rate, thus enabling data communications, and illuminations. LEDs are widely used in everyday infrastructures including homes, offices, street and traffic lights and smartphones as shown in Figure 1.

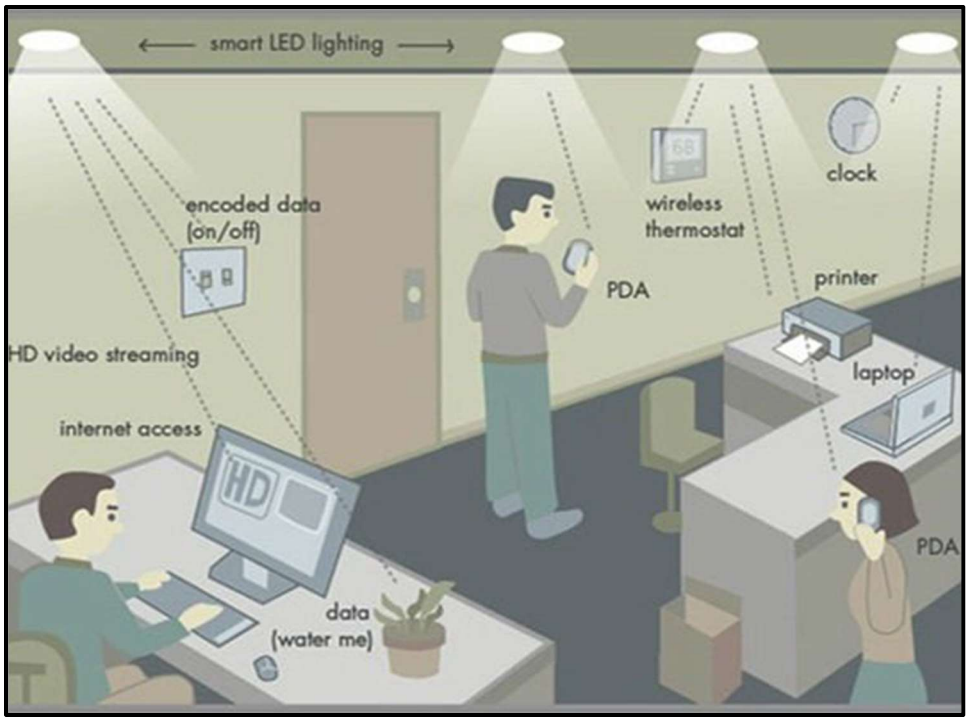

Figure 1. Demonstration of visible light communication[3].

As VLC is directional, it can provide dedicated communication channel confining in a smaller area to reduce the interference [4]. Besides, Internet of Things (IoT) network is becoming more and more important, as many devices can be connected for sensing, monitoring or resource sharing, as shown in Figure 2. A revolution is happening in indoor lighting, as incandescent bulb that has been widely used to light our environment since it was discovered a century ago is slowly eliminated due to its extreme inefficiency. Even in the latest incandescent bulbs, maximum 10% of the electrical power is transformed to useful emitted light. In 1990s, the compact fluorescent bulbs were introduced and achieved popularity in the last decade as they provide more lumens per watt efficiently.

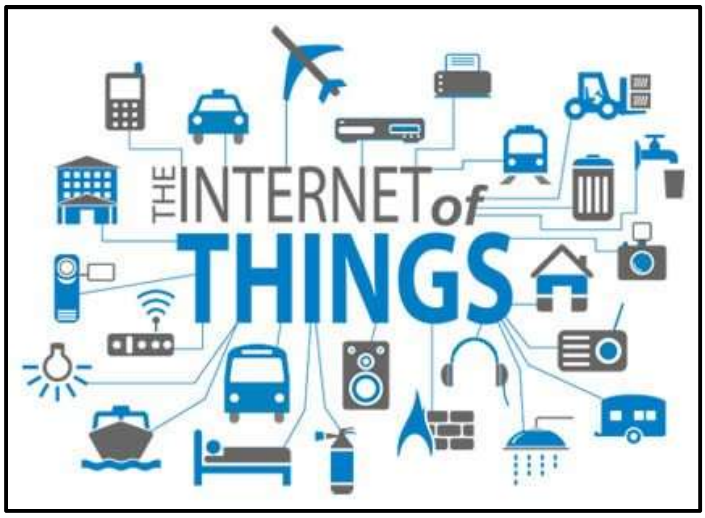

Figure 2. Demonstration of Internet of things[5].

Although, recent updates in solid-state lighting through Light Emitting Diodes (LEDs) have permitted extraordinary energy efficiency and luminaire lifespan. Standard luminous efficacy (how much electricity is used to provide the desired illumination) of first-in-class LEDs is as high as 113 lumens/watt in 2015 [6], and is proposed to be around 200 lumens/watt by the year 2020. Comparably to now a days incandescent and fluorescent bulbs which provide an average luminous efficacy of 15 and 60 lumens/watt [6] respectively, it is a great increase. Correspondingly, the lifespan of LEDs spaces from 25 000 to 50 000 hours obviously higher than compact fluorescent (10 000 hours).

Along with the rapid increase in the usage of LEDs, and contrary to the previous illumination technologies; LEDs have the ability of switching to different light intensity levels at a very fast rate which human eyes cannot percept, and maintain an uncommon opportunity for communication. As encoding the data variously by modulating the emitting light. At the receiver a photodetector (light sensor or a photodiode) or an image sensor

(matrix of photodiodes) can demodulate the signals and decode the data. Aforementioned the LEDs functionally obtain dual purpose illumination as well as communication.

Recent studies showed that VLC is able to achieve very high data rates (nearly 100 Mbps in IEEE 802.15.7 standard and up to multiple Gbps in research). In comparison to existing wireless communication techniques, visible light communication has unique importance. Primarily in the last two decades the current RF spectrum is scarce to cope up with the traffic demand. In consistent to the visible light spectrum which encompasses hundreds of terahertz of license free bandwidth as shown in Figure 3 [7] is totally untapped for communication, and can enhance high-capacity mobile data networks. Secondly, visible light permits the use of small LED transmitter cells with no inter-cell interference problems, due to its high frequency cannot penetrate through most objects and walls, which provide wireless communication security. Thirdly, VLC systems can be utilized cheaply and effortlessly as existing lighting infrastructure will be used for the aim of communication.

The initial visible light communication IEEE standard was proposed in 2011 in the form of IEEE 802.15.7 [7] which embodied the link layer and physical layer design specifications. VLC link achieved a capacity exceeded 1 Gbps recently, and huge research intentions are being directed towards realizing the full potential of VLC.

1.2 Challenges and Motivation

Future generation wireless communication systems, LED's have distinctive features such as low cost, lower power consumption, portability, security [8]. They are

already installed in various lighting applications of our everyday life's lights existing at home, commercial building, display at streets, personal mobile telecommunication devices. So the existing lighting equipments in LED's are being deployed. Various techniques have addressed many challenges facing VLC systems. Such as maintaining connectivity for mobile users, shadowing when line of sight (LOS) link from user to all sources are blocked, and Multiple access for all end users to network simultaneously, symbolic feature of light-Dimming, noise in the VLC atmosphere whether indoor or outdoor.

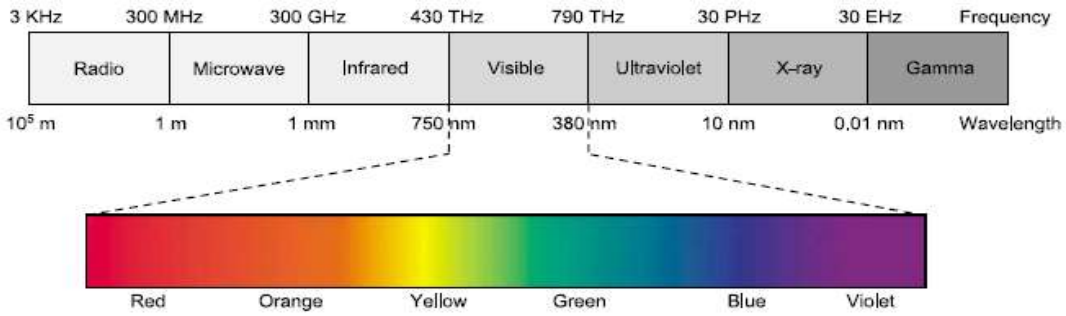

Figure 3. Human eye can perceive the electromagnetic signals between the frequency range of 430 THz and 790 THz which is referred as the visible light spectrum [7].

Wireless visible light communication system is characterized by two influential features high power efficiency and low nonlinear distortion. Sng-Burm, Heung-Gyoon [9] suggested a novel Peak – to – Average Power Ratio (PAPR) reduction approach to mitigate non-linear distortion of LED for reducing PAPR. Moreover, an adaptive inter carrier interference (ICI) suppression algorithm is used in order to boost the performance through enhanced signal to noise power ratio (SNR) by an adaptive channel estimation technique.

A crucial factor that alters VLC system performance received power is unstable with changing White LED lights position, even though the receivers are at the same height in a room. Ding, KeXizheng [10] studied the relationship between the lights platform and

the received power uniformity, and an optimal lights layout design is presented by Ding [10].

On the other hand, Richard, Sridhar [11] focused on other challenges like flicker mitigation and dimming in visible light. Any possible flicker, fluctuation of light brightness, occurring from modulating the light source for communicating must be alleviated, because humans are negatively affected physiologically. The IEEE 802.15.7 presents dimming adaptable techniques for flicker-free and while maintaining high data rates communication [8].

Also the IEEE 802.15.7 standard breaks the spectrum into 7 color bands to offer multiple LED color choices for communication. Therefore, Authors used the principle of Color shift keying (CSK) modulation to define different colors for communication.

Many different approaches expose the VLC using a Digital camera and an LED Flashlight. The direct-able LED flashlight acts as the transmitting device and a digital camera as the receiver. On such approach [12] image processing methods are used to detect the received signal from a saved camera image. It is constructed to work indoors under certain lighting conditions, i.e., overhead lighting and ambient daylight. Since image processing concepts are used, many constraints are taken into consideration for communication, the ambient lighting intensity of the room less than the transmitter light intensity and avoid any highly reflective surfaces.

VLC is also adopted in the outdoor areas, which noise affects it. Paper [13] investigates SNR factor of VLC in outdoor intelligent transportation system (ITS) environment. ITS scales down accidents, congestion, and present smooth flow of traffic.

Additionally, the paper studies the demonstration of VLC in day time in Vehicle-to-Infrastructure (V2I) scenarios, simulating it using a 3D computer build in which two ITS scenario are Vehicle to Vehicle (V2V) and Vehicle-to-Infrastructure (V2I) as shown in Figure 4. The study proves that V2V is difficult compared to V2I cases, and also suggests performing enhancements to the V2V link communication using VLC.

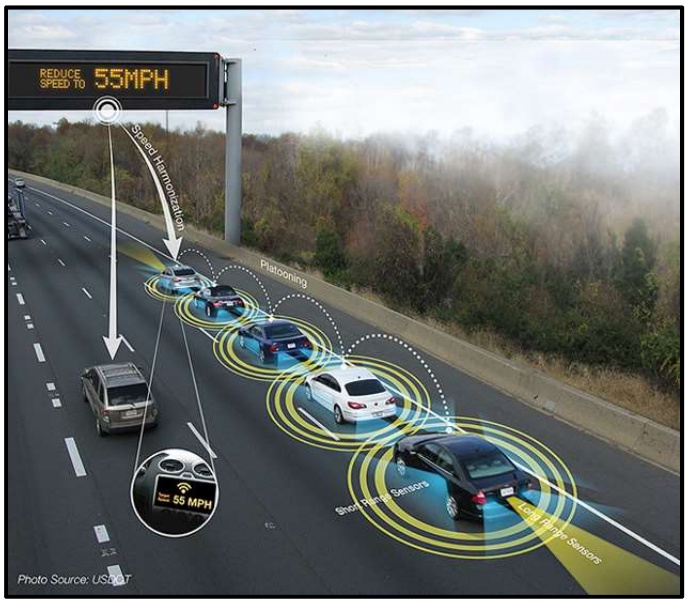

Figure 4. Demonstration of Intelligent transportation system [14].

The optical performance is formed using white LED (WLED) and verified in [15], and phosphor induced white light are subjected on the target area to meet the demands for high optical transmission. There are few constraints that limit VLC, like interference of light. The author studied the interference in the ambient light which degrades the system achievements. However, AVR based models mitigate the noise interference from ambient light.

The current technology used in VLC system is Color-shift-keying (CSK) modulation and code-division multiple-access (CDMA)[16] where the visible light and mobile phones are used as transmitter and receiver, simultaneously as shown in Figure 5 [16]. This approach can maintain multiple users to simultaneously have orthogonal spreading-codes thus each user is given code.

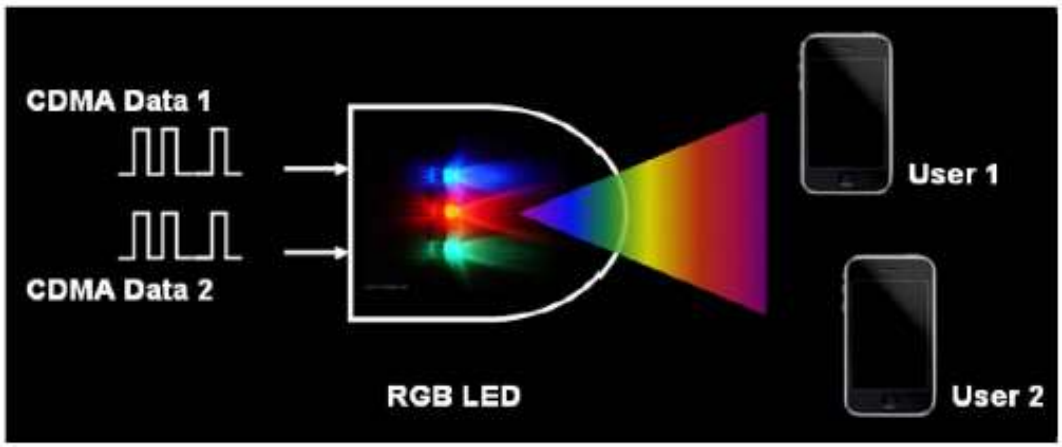

Figure 5. Proposed CSK-CDMA VLC system [16].

1.3 Communication System Block Diagram

Communication systems are designed to send information from a source to one or more destinations. The general communication system block diagram is shown in Figure 6. The information generated by the source may be of the form of voice, a picture, video or plain text in some particular language, then converted into a sequence of binary digits by the source encoder. The channel encoder introduces, in a controlled manner, some redundancy in the binary information sequence which can be used at the receiver to overcome the effects of noise and interference in the transmission of the signal through the channel. The output of the channel encoder is passed to the modulator then transmitted

through the channel which can be wired or wireless medium; such as copper wire, coaxial cable, wave guide, fiber optic cable, antennas and laser or LED. Similarly for the receiver, it can be wired, antenna or photodetector, in case of optical transmission, which will recover the data that will be demodulated and decoded to construct the original data.

This study is focused on the transmitter, channel analysis, and receiver of an optical communication system using visible light communication; LED will act as a transmitter and the photodetector as a receiver.

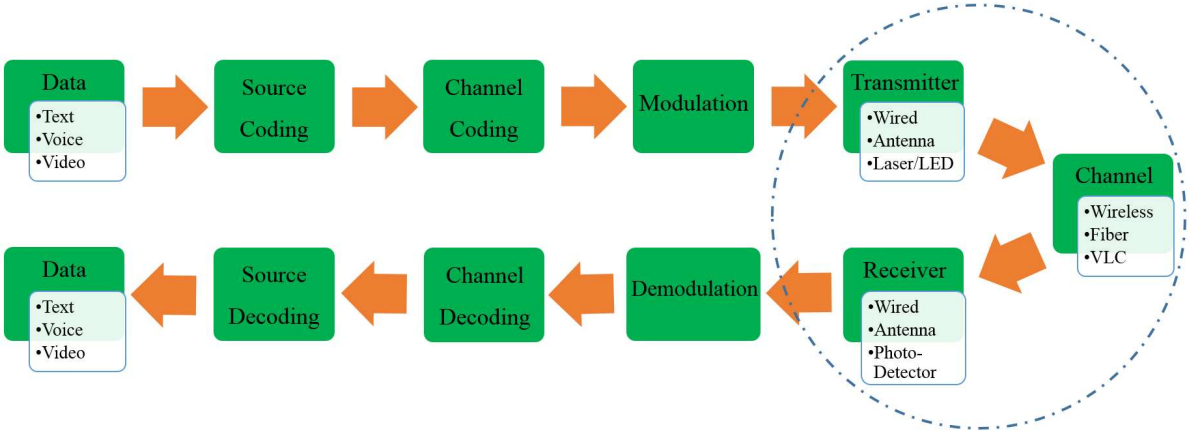

Figure 6. Communication Functional Block Diagram.

1.4 The Proposed Research

In this thesis the proposed improved system model for both indoor visible light communication and intravehicle visible light communication is presented to modify the SNR and power distribution levels. This thesis is organized as follows, chapter 2 shows the IEEE 802.15.7: visible light communication standard, and chapter 3 represents the proposed indoor visible light communication system model, channel transfer characteristics, transmitter, and receiver.

Also the indoor simulation results are shown in chapter 3. Intravehicle visible light communication overview and system model characteristics are discussed in chapter 4 and also the results for the proposed improved model simulation are presented in the same chapter. Moreover, in chapter 5 a VLC system using CSK modulation and CDMA technique concurrently is studied, where mobile-phone camera is used as the receiver (Rx). Finally, a discussion and conclusion are presented in chapter 6.

CHAPTER 2

IEEE 802.15.7: VISIBLE LIGHT COMMUNICATION STANDARD

2.1 Introduction

Visible light communications (VLC) use the visible spectrum wavelengths of 390–750 nm or frequency band of 400–790 THz and offer wireless communication using light-emitting diodes (LEDs).It is viable to transmit data using LEDs without an observable effect on the lighting output and the human eye, because the human eye notices only the average intensity when light changes fast enough. VLC can be used in a various range of short- and medium-range communication applications, which include wireless local, personal, and body area networks (WLAN, WPAN, and WBANs), vehicular networks, and machine-to-machine communication along with many others. In addition to energy efficiency, VLC provide multiple other inherent advantages over radio frequency (RF)-based counterparts, like immunity to electromagnetic interference, operation on unlicensed bands, additional physical security, and a high reuse factor resulting from a high degree of spatial confinement.

The academic interest in VLC is growing, resulting in a rich literature spanning from channel modeling to physical layer design and upper layer issues .Beside of academic interest, industrial attention to VLC has caused related standardization activities to avoid fragmentation of proprietary vendor solutions in this emerging market. In Japan, the Visible Light Communications Consortium (VLCC) (www.vlcc.net) boosted the standardization activities and offered two standards known as the visible light communication system standard and the visible light ID system standard, which were accepted by the Japan Electronics and Information Technology Industries Association

(JEITA) in 2007 and became known as JEITA CP-1221 and JEITA CP-1222, respectively. Recently, in June 2013, they also proposed an enhanced version of the JEITA CP-1222 named as JEITA CP-1223 visible light beacon system standard. Realizing the potential of this emerging technology, the Institute of Electrical and Electronics Engineers (IEEE) produced IEEE Standard 802.15.7, which was approved in June 2011 (IEEE, 2011). The standard describes a physical layer (PHY) and a medium access control (MAC) layer for VLC and guarantees data rates sufficient to accommodate audio and video multimedia services. In this chapter, we first provide an overview of this IEEE standard describing the main features of PHY and MAC layers. The last section is reserved for the most recent standardization activity, which will modify the IEEE Standard 802.15.7.

2.2 Overview of IEEE standard 802.15.7

As personal area network (PAN) is the connection of information technology devices within a short distance. IEEE Standard 802.15.7 presents visible light communication personal area network (VPAN) as its network form. In a VPAN, a coordinator is in charge for starting and maintaining a network, and assigning new devices to an existing VPAN. Also VPANs defined three different network topologies, peer-to-peer, star, and broadcast.

- **Peer-to-peer topology:** The peer-to-peer networking topology is described to support communication between two nodes that ordinarily can be used for both sending and receiving, and act as both a device and a coordinator.

- **Star topology:** For this topology, a coordinator controls the communication network and can connect with all the devices within the network.
- **Broadcast:** The coordinator sends data which will be received by every device in the network. This type of communication is unidirectional, as a result it doesn't involve a destination address.

IEEE 802.15.7 standard examined three classes of VLC devices; infrastructure, mobile (portable), and vehicle. In Table 1, the main specifications of each class are shown.

Table 1. VLC Device Classification

	Infrastructure	**Mobile**	**Vehicle**
Fixed coordinator	Yes	No	No
Power supply	Ample	Limited	Moderate
Form factor	Unconstrained	Constrained	Unconstrained
Light source	Intense	weak	Intense
Physical mobility	No	Yes	Yes
Range	Short/long	Short	Long
Data rates	High/low	High	Low

2.3 MAC Layer

The MAC layer offers two functions accessed through two service access points (SAPs). MAC management is accessed through the MAC link management entity SAP (MLME-SAP), while MAC data are accessed through the MAC common-part sublayer

SAP (MCPS-SAP). The MAC layer executes all access to the physical layer and is responsible for the following tasks:

1. Generating network beacons if the device is a coordinator
2. Synchronizing to network beacons
3. Supporting device association and disassociation
4. Supporting color function (i.e., a function that provides information, such as device status and channel quality to the human eye via color)
5. Supporting visibility to maintain illumination and mitigate flicker
6. Supporting dimming (i.e., reducing the radiant power of a transmitter while preserving the color of the transmitted light)
7. Supporting device security
8. Providing a reliable link between two peer MAC entities
9. Supporting mobility

The standard provides systems to start and maintain a VPAN. The device uses channel scanning to access the current state of a channel, locate all beacons within its operation environment, or detect a specific beacon with which it has lost synchronization. The networks need beacons for synchronization or support for low-latency devices. If the network does not require synchronization or support for low-latency devices, it can choose to turn off the beacon for ordinary transfers. However, network discovery still needs the beacon. Then a channel scan and selection of a proper VPAN identifier, which is not used by any other PAN in the same area, operation as a coordinator starts. The association/disassociation systems to permit the devices to join or leave a VPAN are further explained in the standard.

2.4 PHY Layer

The duties of the physical (PHY) layer are link foundation and termination of a connection to a communications medium. According to the IEEE 802.15.7 standard for VLC, the PHY layer is responsible for the following tasks:

- Activation and deactivation of the VLC transceiver
- Wavelength quality indication (WQI)
- Clear channel assessment
- Data transmission and reception
- Error correction
- Synchronization
- Supporting dimming

Based on the intended data rate and usage environment, the IEEE 802.15.7 standard includes a number of various PHY layer types:

- **PHY I:** In his type on–off keying (OOK) and variable pulse position modulation (VPPM) are used. It handles concatenated coding with Reed–Solomon (RS) and convolutional coding (CC). This PHY type is designed for outdoor low data-rate applications with rates in the tens to hundreds of Kbps.
- **PHY II:** Similar to PHY I, PHY II uses OOK and VPPM but with higher optical clock rates intending to achieve higher data rates in the tens of Mbps. But It only supports RS coding. This PHY type is for indoor operation with moderate data rate applications. PHY I and PHY II also support a run-length limited (RLL) code to maintain DC balance, clock recovery, and flicker mitigation.

- **PHY III:** This type is designed for applications with multiple light sources and detectors. It operates using CSK and RS coding. The desire of this type is to achieve data rates in the order of the tens of Mbps.

All operating modes are listed in Table 2.Any IEEE 802.15.7-compliant device must assign at least one of the PHY I and PHY II types. For coexistence a device using the PHY III type should also implement PHY II mode. Also the PHY types may work in the existence of dimming. As OOK under dimming condition maintains constant range and variable data rate by embedding compensation time. However, VPPM under dimming maintains constant data rate and variable range by altering the pulse width. More specifications on the optical clock rates, data rates, and error correction codes for each PHY type are illustrated in Table 2. As shown in table 2, multiple optical rates are presented for all PHY types in order to assist a broad class of LEDs for different applications. The MAC layer chooses the optical rate used for communication during device discovery.

Table 2. VLC Device Classification

				FEC		
	Modulation	RLL Code	Optical Clock r	Outer Code (rs)	Inner Code (cc)	Data Rate
PHY I	OOK	Manchester	200 KHz	(15,7)	1/4	11.67 Kbps
				(15,11)	1/3	24.44 Kbps
				(15,11)	2/3	48.89 Kbps
				(15,11)	None	73.3 Kbps
				None	None	100 Kbps
	VPPM	4B6B	400 KHz	(15,2)	None	3556 Kbps
				(15,4)	None	71.11 Kbps
				(15,7)	None	124.4 Kbps
				None	None	266.6 Kbps
PHY II	VPPM	4B6B	3.75MHz	(64,32)	None	1.25 Mbps
				(160,128)	None	2 Mbps
			7.5 MHz	(64,32)	None	2.5 Mbps
				(160,128)	None	4 Mbps

				None	None	5 Mbps
	OKK	8B10B	15 MHz	(64,32)	None	6 Mbps
				(160,128)	None	9.6 Mbps
			30 MHz	(64,32)	None	12 Mbps
				(160,128)	None	19.2 Mbps
			60 MHz	(64,32)	None	24 Mbps
				(160,128)	None	38.4 Mbps
			120 MHz	(64,32)	None	48 Mbps
				(160,128)	None	76.8 Mbps
				None	None	96 Mbps
PHY III	4-CSK		12 MHz	(64,32)	None	12 Mbps
	8-CSK			(64,32)	None	18 Mbps
	4-CSK		24 MHz	(64,32)	None	24 Mbps
	8-CSK			(64,32)	None	36 Mbps
	16-CSK			(64,32)	None	48 Mbps
	8-CSK			None	None	72 Mbps
	16-CSK			None	None	96 Mbps

2.5 Recent Activities in IEEE standardization

In 2013, the IEEE 802.15 working group (WG) created a study group to determine if an amendment to the standard is needed. The group discussions and suggestions from industry and academia indicated a project authorization request which states:

This amendment explains a physical layer (PHY) … using light frequencies over the spectral range of 10,000 nm (infrared [IR]) to 190 nm (near ultraviolet [UV]) and any MAC changes exactly required to aid this PHY. Transmitting devices carry such sources as displays, commonly found on cameras and mobile devices, and other LED based sources such as flashes, flashlights, LED tags, and LED/laser sources. (IEEE P802.15.7r1, 2016)

As IEEE Standards Association accepted the project authorization request, the IEEE 802.15 WG are able to work on a new standard which is open to almost any type of VLC communication. For prospective standard proposals (Janget al, 2015), a technical

requirements document has been prepared for guidance, which uses the term optical wireless communication (OWC) and classifies OWC into:

- Image sensor communications
- Low-rate photodiode communications
- High-rate photodiode communications

Considering the definition of low speed and high speed, the throughput threshold data rate is 1 Mbps as measured at the PHY layer output of the receiver. Any throughput less than 1 Mbps rate is considered low rate and higher than 1 Mbps is considered high rate. The group decided the feasible applications that can be served by each communication type. Image sensor communications enable OWCs using an image sensor as a receiver. Main applications of image sensor communications are listed as:

- Offline to online marketing/public information system/digital signage
- Internet of Things (device-to-device/Internet of light [IoL])
- Location-based services/indoor positioning
- Vehicular communication/vehicular positioning
- Underwater communication
- Point-to-(multi)point/relay communication

Low-speed photodiode receiver communications, which is a wireless light ID system using various LEDs with a low-speed photodiode receiver, can be used in the below applications:

- Underwater/seaside communication
- Point-to-(multi)point/communication
- Digital signage
- Internet of Things (device-to-device/Internet of light [IoL])

- LOS authentication
- Identification based services

The high-speed photodiode receiver communications is high-speed, bidirectional, networked, and mobile wireless communications using light with a high-speed photodiode receiver. Main applications for high-speed photodiode receiver communications are:

- Indoor office/home applications (conference rooms, general offices, shopping centers, airports, railways, hospitals, museums, aircraft cabins, libraries, etc.)
- Data center/industrial establishments, secure wireless (manufacturing cells, factories, hangers, etc.)
- Vehicular communications (vehicle-to-vehicle, vehicle-to-infrastructure)
- Wireless backhaul (small cell backhaul, surveillance backhaul, LAN bridging)

The group was assigned another task to determine if a channel model is necessary to compare different standard proposals. The group decided that all proposals which include the PHY algorithms for the high-rate PD communications must use the channel impulse responses provided in TG7r1 Channel Model Document for High-rate PRD Communications (Jang et al. 2015) for the specific scenario that they intend to address in their proposal. The exact channel impulse responses are provided in TG7r1 CIRs Channel Model Document for High-rate PD Communications (Uysal et al. 2016). The task group aimed to receive proposals for each type of OWC in 2016; the planned finalization date of the standard is 2018.

CHAPTER 3

INDOOR VISIBLE LIGHT COMMUNICATION

3.1 Propagation Modes

Six different configurations have been illustrated in [17] for indoor links, mostly classified based on the existence/nonexistence of the line of sight (LOS) link between the transmitter Tx and receiver Rx. Considering LOS structure, which is the most essential, the emitter beam angle and the receiver field-of-view (FOV) will determine the transmission channel. As for the case of directive links, the Tx and Rx have a small divergence angle and FOV, respectively correspondingly need very accurate alignment and suffer from blocking due to the movement of people or existence of objects within the room. While the so-called hybrid links, Tx and Rx have various degrees of directionality[17]. In nondirective links, Tx and Rx both have a wide angle. Regarding diffuse configuration; one of the most popular and widely used schemes; the source position plays greatly affects the power levels at different points within a room. In this scheme, the Tx pointing up toward the ceiling has a wide beam angle and the Rx has a wide FOV, as a result collects reflected diffused light from the ceiling, floor, walls, and objects in the room[18].

Generally, to provide high data rate links, the presence of an LOS path is a must since on directed LOS or diffused configurations will reduce the achievable data rate[19]. Certainly, the LOS assists in having a much higher received light intensity; resulting in higher signal-to-noise ratio (SNR) that can be used to increase the data rate and also alleviate the risk of inter symbol interference (ISI), but at the trade of limited mobility or possibility of shadowing/beam blockage.

3.2 Channel Simulation

The optimal LOS channel impulse response (CIR) is basically a time delayed and scaled delta function showing amplitude degradation of the transmitted signal. Hence, the link attenuation becomes an essential factor which can be derived from the photometric parameters mostly adopted for formalization of LED illumination capability. For the aim of performance interpretation of VLC systems, one may attend to experimental measurements [14,15] or to numerical simulation of the propagation channel. The later technique is faster and cost efficient moreover it can also be helpful prior to the experimental verifications. The propagation channel is totally defined by the CIR. For any link configuration, the CIR has to be determined at various positions within the indoor environment. By then, it is obligatory to have an accurate and computationally efficient simulation method.

The number of reflections from walls and other objects within the room is the most crucial point in the simulation, which will take time depending of course on the number of reflections taken into consideration. The surface reflection characteristics within an indoor environment rely on various factors including the material, operating wavelength of the light source, and the angle of irradiance. The smoothness or roughness of the surface in regard to the wavelength will also influence the shape of the reflected patterns. As a smooth surface like a mirror or a shiny object reflects the incident beam only in one well-defined direction (i.e., specular reflection), however a rough surface reflects the beam in random directions (i.e., diffuse reflection). In real life, most reflections are commonly diffuse in nature where the Lambertian model can properly be used[16,17]. Several measurement

campaigns have validated the basic diffuse reflection model, illustrating the importance of the orientation of Tx and Rx as well as the importance of shadowing. There have been several proposed approaches to simulate the diffuse light components. In [18], it was proposed to decompose the room surface into a number of reflecting elements, which scatter the light according to the Lambertian model, and to sum the reflected light from all these elements at the Rx. However, only single reflections were considered in this method. A development of the approach of [18] to consider higher-order reflections was proposed in [22] applying a recursive algorithm. This technique has been extensively used in the literature; though, it suffers from high computational complexity.

Despite of most of these approaches used the infrared (IR) transmission rather than VLC. The major difference for IR communications, a narrowband near-monochromatic IR light source is used and a constant reflectance is considered for the reflectors, independent of the wavelength [23]. On the other hand, VLC systems use phosphor-based white LEDs with emission in the visible spectrum (from 380 nm to 780 nm) to alleviate fabrication complexity and cost, in comparison to red, green, and blue (RGB)-based white LEDs, as all three colors are transmitted simultaneously. However, the bandwidth of the phosphor-based LEDs is very limited (normally several MHz), due to the slow time constant of the phosphor. A different method is to use a narrowband blue filter at the receiver in order to filter out the slow yellow component to enhance the modulation bandwidth of the LED [20, 21]. Since we effectively work in the narrowband, most of the outcomes of the work done in the IR band can be exploited. For now, it is noticeable that the reflectivity of the IR band is higher than that of the visible band [26]. As for, VLC channel characterization depending

on the recursive algorithm of [17] is studied in [20, 23] where constant reflectance was examined. [23]studied when the white light is directly used for signal transmission and detection, as we need to adapt the channel model to take into consideration the wavelength-dependent nature of reflectors. Moreover the wideband nature and power spectral distribution of the visible light source are considered. Certainly, if the number of reflections considered in the simulations is not too high, as an acceptable approximation, the average reflectivity over the entire visible spectrum can be applied [19, 24] .

3.3 General Transmission Link Model

Similar to most optical wireless communication (OWC) systems, VLC system uses intensity modulation with direct detection (IM/DD) [17], as it reduces cost and implementation complexity. By that, the intensity of the LED, x(t), is modulated by the input signal. Defining the photocurrent generated by the Photodetector (PD) at the receiver by y(t), the baseband equivalent of the optical link is explained by (see Figure 7):

$$y(t) = Rx(t) \otimes h(t) + n(t) \tag{3.1}$$

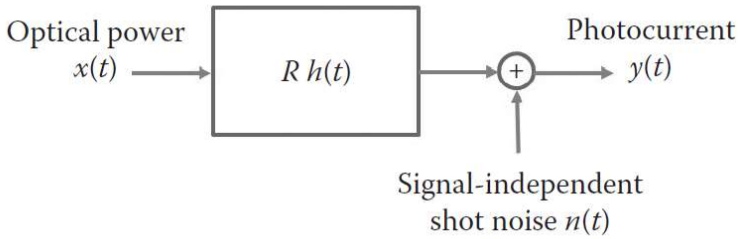

Figure 7. Baseband-equivalent model of the optical link with IM/DD.

where R is the PD responsivity, h(t) is the baseband CIR, $\otimes$ denotes convolution, and n(t) is the additive white Gaussian noise. x(t) is nonnegative as it represents optical intensity. The receiver noise n(t) is primarily due to the ambient light and in the form of shot noise. The main causes of ambient noise are sunlight and artificial light like that of incandescent and fluorescent lamps [26, 27]. Moreover, the power spectral density of different ambient light sources and that of the corresponding electrical signals are in [17]. Throughout daytime, sunlight passing through windows is mainly stronger than the other two sources. Even, if LEDs are completely deployed for indoor lighting, our only concern is the sunlight. However, discrete multitone techniques (DMT) is used to reduce the interference from fluorescent lighting[24]. The generated shot noise due to ambient light can weaken the performance of the VLC system. Consider that in the case where the blue light is used at the receiver for signal detection by narrow spectral filtering, the effect of ambient light is generally diminished. Then the dominant noise source is the receiver preamplifier thermal noise if the ambient light is neglected.

3.4 Indoor Communication System Model

VLC system consists of line of sight (LOS) and diffused channel. This system model consider only LOS channel, and study the transmission of data through the air to the receiver.

A. Transmitter and Visible Light Channel

The channel transfer function for white LED light source directly pointing in the direction of optical receiver is given by [31]:

$$H_{LOS} = \begin{cases} \frac{A_{rx}}{h^2} R(\emptyset) \cos(\varphi) & 0 \le \varphi \le \varphi_c \\ 0 & \varphi > \varphi_c \end{cases} \quad (3.2)$$

where A_{rx} is the detector area, h is the distance between the transmitter and the receiver, φ is the angle of incidence,φ_c is the photodiode's field of view (FOV) [31].$R(\emptyset)$ is Lambertian radiant intensity of LED known as:

$$R(\emptyset) = \left[\frac{n+1}{2\pi}\right] cos^n(\emptyset) \quad (3.3)$$

$$n = -ln2/\ln(\cos \emptyset_{\frac{1}{2}}) \quad (3.4)$$

where n is Lambertian emission coefficient, associated with semi-angle at half power $\emptyset_{\frac{1}{2}}$. (3.4) expresses the total received power for only LOS channel:

$$P_{LOS} = \sum_{i=1}^{LED_{num}} P * H_{LOS} \quad (3.5)$$

P is the total transmitted power and P_{LED} is the LED power:

$$P = P_{LED} * R(\emptyset) \quad (3.6)$$

B. Receiver

The receiver is consisted of photodiode, concentrator and optical filter, as a consequence the received power for LOS channel is [31]:

$$P_{re} = P_{LOS} \times g \times T \quad (3.7)$$

where g is the concentrator gain, T is the optical filter's transmission coefficient. Photodetector will convert light signals to electrical signals and the SNR is indicated as:

$$SNR = \frac{i^2}{\sigma^2} \tag{3.8}$$

where σ^2 is the total noise variance and i is the photodiode's output current and are shown as [31]:

$$\sigma^2 = \sigma_{sh}^2 + \sigma_{am}^2 \tag{3.9}$$

$$i = P_{re} \times r \tag{3.10}$$

$$\sigma_{sh}^2 = 2(P_{re} + P_n) \times q \times r \times B_n \tag{3.11}$$

$$B_n = I_1^2 R_b \tag{3.12}$$

$$\sigma_{am}^2 = i_{am}^2 B_a \tag{3.13}$$

where σ_{sh}^2 is the shot-noise variance, $\sigma_{am}^2$is the amplifier noise variance, r is the photodiode response rate, P_n is the ambient light's noise power, B_n is the noise bandwidth, $I_1$is noise bandwidth factor, R_b is data rate, i_{am}^2 and B_a are the amplifier noise density and the amplifier bandwidth, respectively.

C. Differential Optical Receiver

Modified optical receiver can cancel the ambient noise, two photodetectors are cross coupled as shown in Figure 8. The optical signal is transmitted only into one of the receivers. With all other signals being canceled out, the optical signal is an overwhelmingly dominant signal, which is then demodulated and decoded by means of code correlation [32]. Resulting in the change of the shot-noise shown in (3.11) to:

$$\sigma_{sh}^2 = 2P_{re} \times q \times r \times B_n \tag{3.14}$$

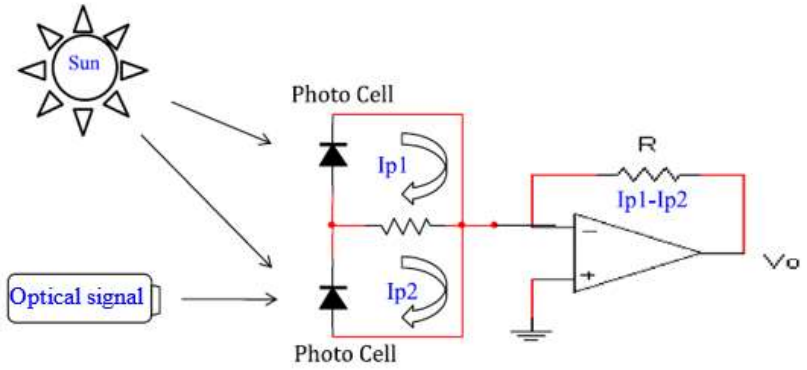

Figure 8. Differential optical receiver, illustrating sun light cancellation; Ip1 and Ip2 are photocurrents due to ambient light and optical signal, respectively[32].

The simulation results to the indoor system model while considering LOS channel and the optimized proposed model results to maintain uniform power distribution with higher power levels are shown in section 3.5.

3.5 Results

3.5.1 Received Optical Power Distribution

A visible light indoor communication system model uses LED lights as four LEDs evenly distribution on the ceiling of the room is shown in Figure 9. In this system model, white LEDs emission high frequency light waves contains modulated signals, which transmit through the air to the receiver, lighting at the same time to complete the wireless transmission of data.

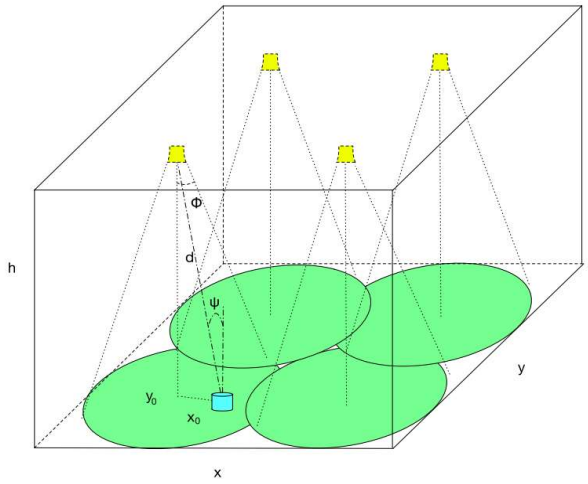

Figure 9. Representation of a room with four LEDs and their footprint [33].

Based on the parameters of table 3, the optical power distribution of LOS channel is shown in Figure 10. According to the analysis in section 3.4, the optical power distribution is almost uniformly distributed around the center with a maximum power of 2.2 dBm and a minimum power of −2.3 dBm. However, depending on the half angle, such uniform power distribution is not possible to achieve with high power levels.

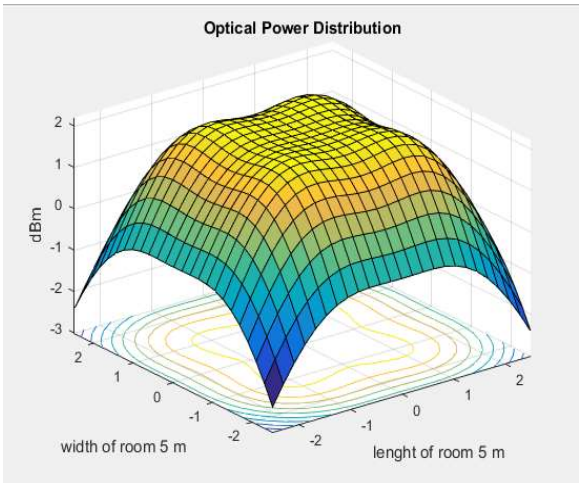

Figure 10. Optical power distribution in received optical plane for a FWHM of 70°

Thus, we simulated the optical power distribution with the semi angle, full width half maximum (FWHM), of 35°. The results of this simulation shown in Figure 11 illustrate the achievement of a maximum power of 4.4 dBm and a minimum power of −2.3 dBm. Nevertheless, the uniform distribution in the previous discussed work does not exist anymore, the optical power level at the center reaches 3.2 dBm which is higher than the maximum of the previously discussed simulation.

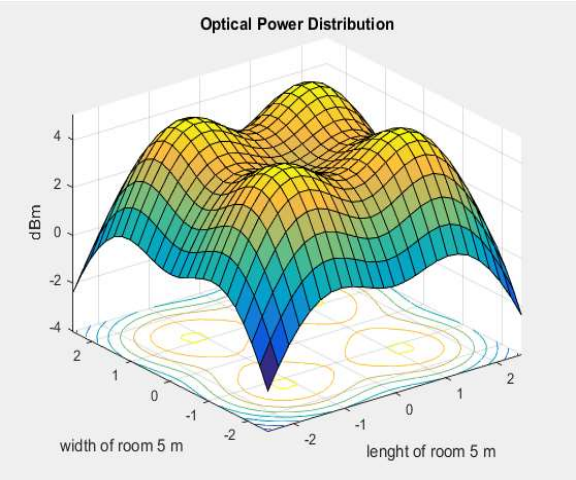

Figure 11. Optical power distribution in received optical plane for a FWHM of 35°.

Table 3. Main Simulation Parameters

System Parameters for a VLC Link		
Room	Size	5×5×3 m3
Source	Location (4 LEDs)	(1.25,1.25,3),(1.25,3.75,3), (3.75,1.25,3),(3.75,3.75,3)
	Semi angle at half power (FWHM)	70º,35º
	Transmitted power (Per LED)	20mW
	Number of LEDs per array	60*60 (3600)

	Center luminous intensity	300-910 lx
Receiver	Receive Plane above the floor	0.85 m
	Active area (A_{rx})	1 cm2
	FOV	60º
	Amplifier Bandwidth B_a	50 MHz
	Concentrator Gain g	6.0
	Photodiode responsivity r	0.4 A/W
	Amplifier noise density i_{am}	5 $pA/\sqrt{Hz}$
	Ambient noise power P_n	19.272 µW
	Noise bandwidth factor I_1	0.562
	Optical filter's transmission coefficient T	1.0

3.5.2 SNR Using Differential Optical Receiver

Similarly referring to the analysis in section 3.4, Figure 12 [31] shows the simulation results of the previously mentioned research work. Where, the received SNR level varied between a min of 82 dB to 87dB.

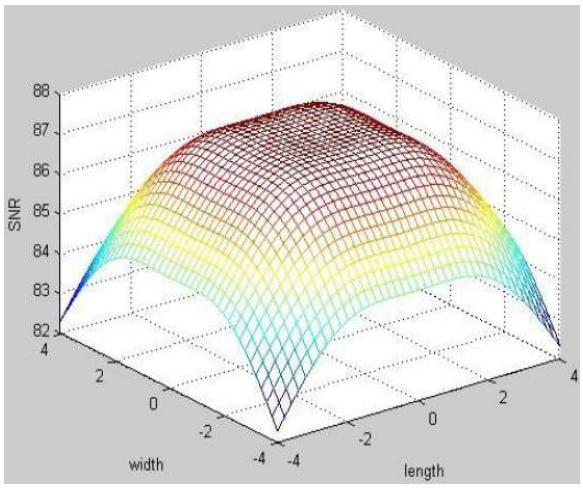

Figure 12. The SNR of receiver without optimization [31].

By using the differential optical receiver along with changing the FWHM to 35º instead of 70º, the simulation results of the proposed model at 10Mb/s bit rate shown in Figure 13 illustrate an output SNR varying between 83 dB to 97.2 dB accompanied by a mitigation of the ambient noise.

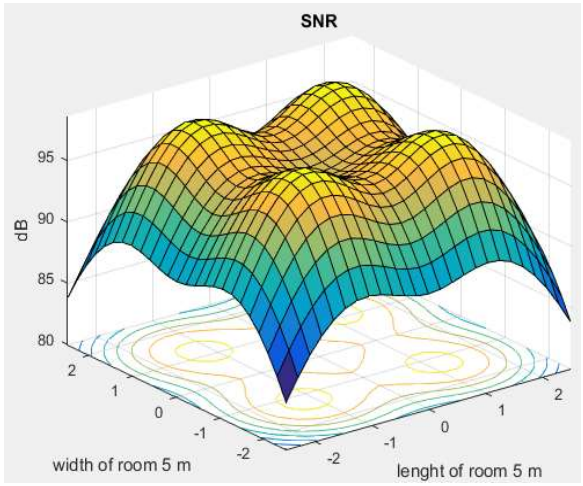

Figure 13. The SNR of receiver with optimization.

Despite both systems, previous research work and proposed model, satisfy the SNR level, 15.6 dB [34], of a communication system at 10^{-6} bit error rate (BER), the proposed model shows better SNR performance of a maximum of 97.2 dB instead of 87 dB.

CHAPTER 4

INTRAVEHICLE VISIBLE LIGHT COMMUNICATION

4.1 Introduction

Recently it was highlighted that optical wireless communication (OW) may provide a compatible solution to the concept of intra-vehicular communications. For example irradiating the interior of the vehicle with infra-red (IR) radiation to serve as a communication link between anything from simple user-vehicular interface devices such as window or air conditioning controllers, to more advanced vehicular technologies such as audio-visual (AV) entertainment units or computer consoles[34]. The advantages to implementing an OW system within a vehicle or Vehicle Ad-hoc Network (VANET) [35], [36] include mitigating against the highly prevalent radio frequency interference [34] and a reduction in costs due to utilizing unregulated spectrum and not having to design a system around other competing RF systems. There is also a potential to save energy in terms of reduction in wired devices that are typically copper cabled and finally a potential to improve manufacturing efficiency should such cabling be removed.

However, before any OW based intra-vehicle communication system is prototyped or developed, it is typically customary for a designer to complete some form of channel analysis. Therefore in this paper, the first kind of such an analysis is presented for the received power based upon a single IR LED source situated upon the ceiling of a Sports Utility Vehicle (SUV). It is shown that several areas of the vehicle are illuminated with sufficient IR power, that intravehicular OW communication is viable.

4.2 Vehicular Structure

To investigate, the OW system is considered to be deployed within an SUV with an internal structure consisting of seats, floors, ceiling and steering wheel etc. with an internal dimension structure of 3.5×1.6×1.5 m3 as shown in Figure 14[37]. In this VLC simulation model we will optimize the received power level and SNR based on the change of FWHM of the LED and ambient noise cancellation using Lambertian radiant intensity model.

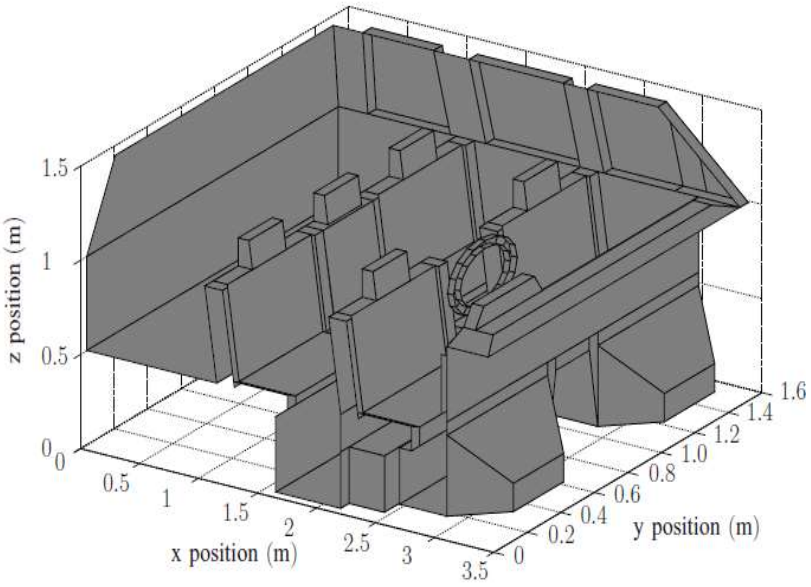

Figure 14. Front facing view of the deployment structure with the driver side wall, windscreen and ceiling removed [37].

Previous work in modelling of intravehicular optical wireless communication system, invisible IR LED was used therefore a strong specular IR reflection model was used, Phong reflection model [37]. It discovered that the rear passengers can, from the linearly scalable 1W source, reach 49μW of received power as shown in Figure 15. As well

as a power up to 16μW may be received on the headrests of the front seats, where audio visual (AV) entertainment units and computer consoles may be located as in Figure 16[37].

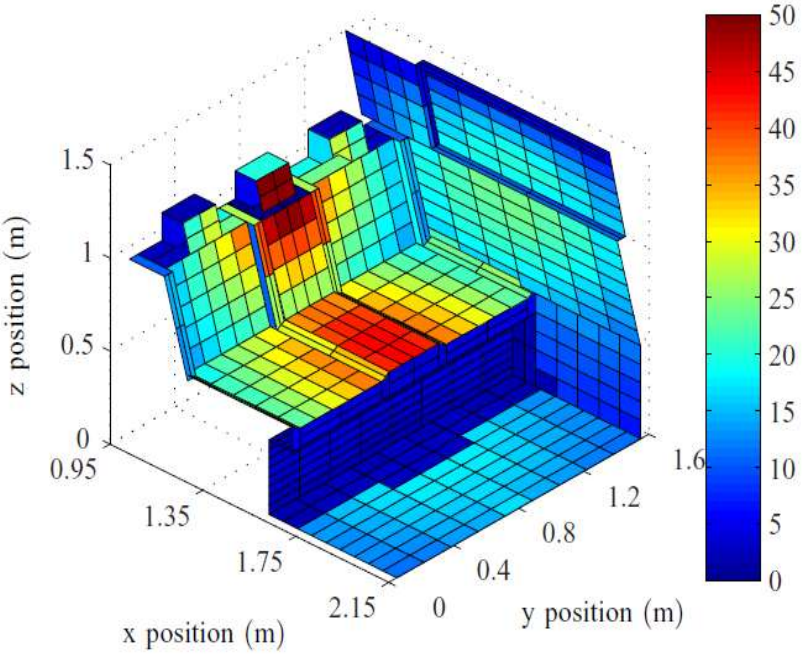

Figure 15. Received power in μW for the driver and front passenger seats[37].

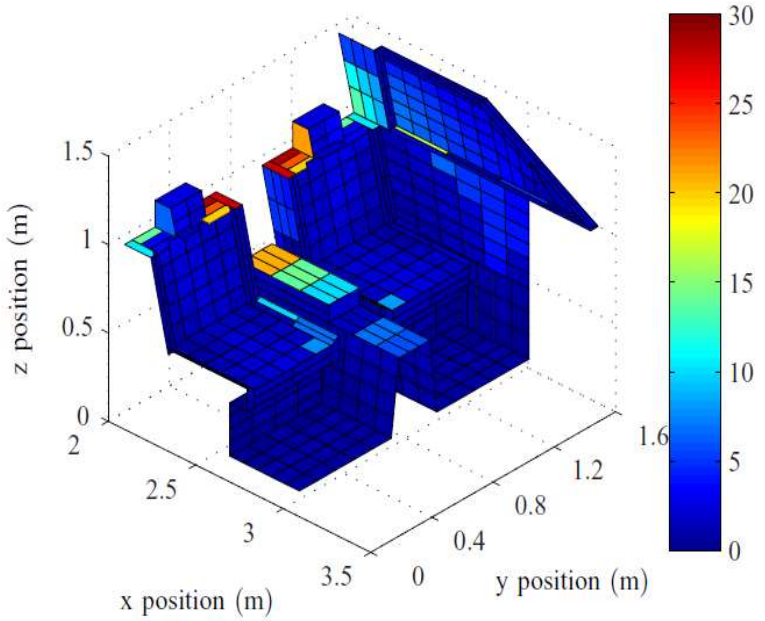

Figure 16. Received power in μW for the rear passenger seats [37].

4.3 Source, Receiver and Lambertian Model

Initially the simplest possible system configuration similar to the indoor room model with considering the new dimensions, the transmitter source is located centrally upon the vehicle ceiling with position vector [1.6, 0.8, 1.5], and Lambertian radiation profile R(∅) is given by equation (3.3). It should be noted that this VLC model only considered the outer dimensions of the SUV cabin structure without the interior seats and the presence of passengers.

The simulation results for the received optical power distribution and SNR are formulated upon the parameters and the equations in chapter 3. However the SUV dimensions are considered rather than the dimensions of the room, along with the location of a single LED source with number of LEDs per array = 50 to maintain 1W source power, and a change in the distance between the transmitter and the receiver to 1m.

4.4 Results

Obviously, the use of visible light source with the optimized characteristics used in the previous room model resulted in more than 100 times the power level of the system .As the proposed model power distribution received for the rear and front seats improved to 7 mW and 8 mW, respectively as shown in Figure 17. Let us compare by considering the received power shown in Figure 17 throughout the rear passenger seats as shown in Figures 15, 16 respectively. Here a maximum received power of 8 mW can be seen to be situated on the middle headrest instead of 49 μW. Furthermore, the left and right headrests can receiver powers between 3 mW and 5 mW rather than 22μW and 28 μW. These areas, with relatively high power are useful for portable devices near the passengers head such as for example, wireless IR headphones or hands free voice equipment. Previously, the lower

section of the back seat is subject to IR radiation with a power ranging between 19μW and 43 μW instead of 4 mW to 7 mW.

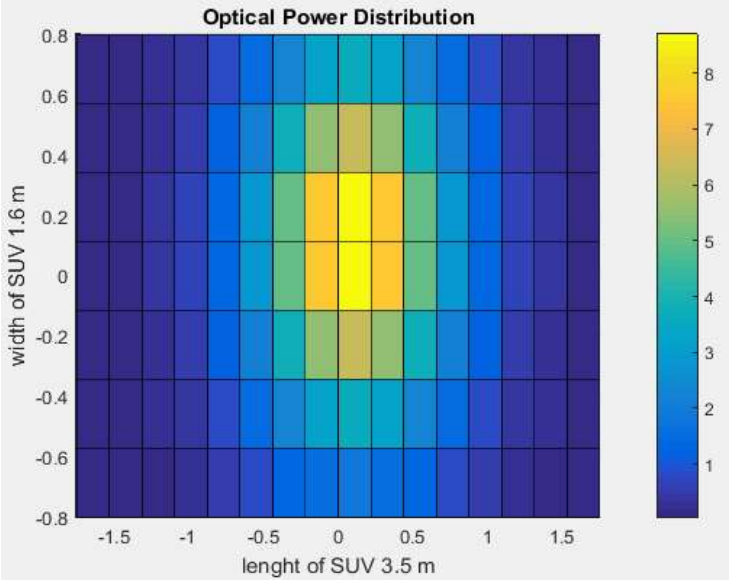

Figure 17. Optimized received power in mW for the rear and front passenger seats.

Personal electronic devices such as mobile phones, laptops, hand-held computer console's etc. would be adequately served in these locations. On the interior door panels, the receiver power ranges from 1 mW to 3 mW. This area with these channel performance attributes, is more than suitable to deploy simple vehicular-passenger interface panels such as window, air-conditioning, heating or AV controllers.

Considering the front seats, the highest area of received power can be found on the middle armrest between the driver and the passenger with a magnitude of up to 20 μW previously and up to 6 mW in the proposed work. This region of the car is both useful to the rear passengers, potentially as a location for resting portable equipment or housing AV sources or consoles.

The other main area of interest, in this view of the car, is around the window sills, where for example, window or wing mirror controllers, heating or other simple user interface switches may be located. Here, a reasonably high level of received power, up to 16 μW in previous work and up to 3 mW in this simulation shown in Figure 17.

Moreover as mentioned in section 3.4, the analysis for receiver SNR output obtained is very spectacular. As shown in Figure 18. 57~ 87.2 dB is achieved assuring the feasibility of VLC intravehicle performance with addressing all the user constraints and needs.

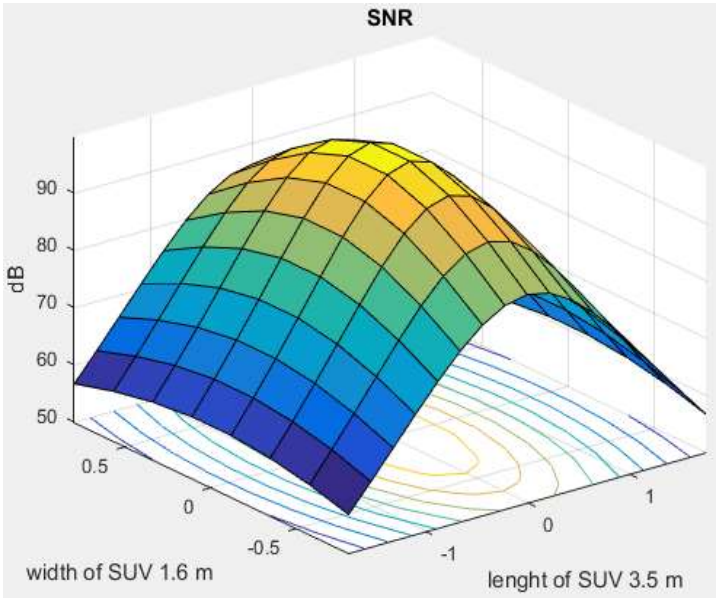

Figure 18. The SNR of receiver for the rear and front passenger seats.

CHAPTER 5

COLOR SHIFT KEYING

5.1 Introduction

Color shift Keying (CSK) is an exceptional modulation technique in VLC systems. Commonly VLC systems use a blue light-emitting-diode (LED) and a yellow phosphor layer on LED(s) which changes the blue light into white. However, the phosphor layer limits the maximum modulation frequency as it has a long relaxation time. By using RGB (red, green, and blue) LEDs the frequency limit can be canceled from the system. Since RGB LEDs are more expensive and need a complex control circuit to form white light, nowadays RGB LEDs are barely used in commercial devices. CSK modulation designs are constructed to work with RGB LEDs in order to achieve higher order, spectrally efficient modulation. While preserving an average perceived chromaticity, data are sent on the instantaneous color of the RGB triplet.

The color-based modulation of CSK has various advantages over intensity modulated techniques. Absence of flicker is assured at all frequencies as the emitted light is regular. The constant luminous flux of the source results in near constant current drive, which consecutively involves a reduced inrush current when modulating data, strong signal isolation from the power line and less inductance caused by large switching currents. Both the symbol rate and the number of color points on the constellation determine the bit rate. In other words the frequency response of the LEDs doesn't limit the CSK bit rate. However, phosphor- based visible LEDs are more often used than RGB LEDs in lighting systems and they are not suitable for CSK.

In CSK standard IEEE 802.15.7, three LEDs are used in the CSK system. Despite, many papers examined the four LEDs CSK systems as an improvement of these systems. Four colors afford a larger color band in the CIE 1931 color space, in turn increases the distances between symbol points, and the constellation can be like M-QAM. The PHY III layer supports CSK modulation in the IEEE 802.15.7. Table 4 shows the different modulation schemes, the error corrections, and the applied clock frequencies[38]. Most CSK devices have to support the 12 MHz clock frequency. The devices send their parameters (e.g., which color bands are supported) to a coordinator, which selects one color channel, that will be used for CSK communication. PHY II layer is used for this handshaking communication. The incoming data are scrambled to alleviate the error effect on the transmission. The scrambled data are usually encoded with RS (64, 32), except for the two highest data rate, where forward error correction (FEC) is not used.

Table 4. The Operation Mode of PHY III Layer.

Modulation	Clock (MHz)	FEC	Data Rate (Mb/s)
4-CSK	12	RS(64,32)	12
8-CSK		RS(64,32)	18
4-CSK	24	RS(64,32)	24
8-CSK		RS(64,32)	36
16-CSK		RS(64,32)	48
8-CSK		None	72
16-CSK		None	96

CSK[39]; an encouraging modulation technique specifically for RGB LED VLC system; can enhance the VLC system capacity and data rate by increasing the bit per symbol rate. Also it can mitigate the single color interference. In consideration of Code division multiple access (CDMA) technology, multiple users can access the network simultaneously[40]. In [16], a VLC system using CSK modulation and CDMA technique concurrently was proposed. Mobile-phone camera is used as the receiver (Rx).

Figure 5[16]. The CDMA data1 adds to the CDMA data2 to create the CSK signal. The CSK signal is sent by an array of RGB-LED. User1 and user2 receive the CSK signal by two different mobile-phone cameras. Individually each user then decodes the data by its own CDMA spreading code. As illustrated on Table 5[16], the CSK consists of 4 color magnitude subsets. Since the number of bit used for each color (color depth) is 8 bits, the magnitude levels represented by of the R, G, and B color are within the range of 0-255. As result of the 24 bits total color depth, RGB can represent 16 777 216 colors or magnitude levels. For instance, in Table 5[16], Color1 (red, green, blue) is represented with magnitudes of (60, 40, 0). So as transmitter (Tx) emits Color1 magnitude subset (R: 60, G: 40, B: 0), data logic bits of 00 are transmitted.

Table 5. Bit Map of Color Magnitude Subsets[16].

Bit Map		**Color Magnitude Subset**		
		Red (R)	**Green(G)**	**Blue (B)**
Color1	**00**	60	40	0
Color2	**01**	40	0	40
Color3	**10**	20	20	60
Color4	**11**	0	60	20

5.2 Design of Tx and Rx in CSK-CDMA VLC System

The design of the suggested Tx and Rx in CSK-CDMA VLC system is shown in Figures 19 and 20[16]. For an example, Tx transmits Color1 to User1 and Color2 to User2 simultaneously, which are bits "00" to User1 and bits "01" to User2. In color1 the value for the red is 60 as shown Figure 19, which is spread by spreading code1 [1, -1, 1, -1]] and the Spread-signal1 becomes [60, -60, 60, -60]. However, for Color2 the red value is 40 and spread by Spreading code2 [1, 1, -1, -1] resulting in [40, 40, -40, -40] as the spreading signal2.

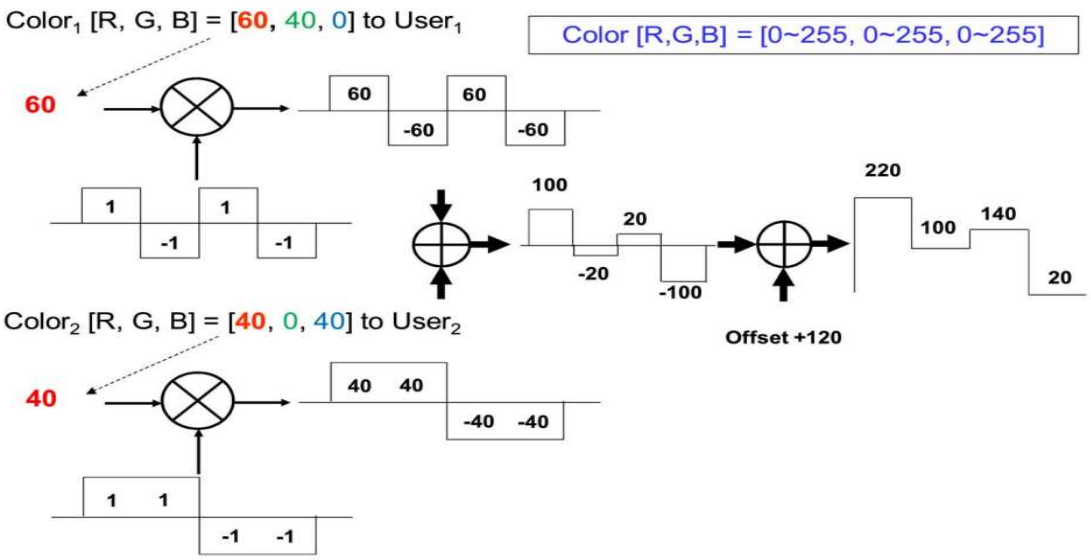

Figure 19. Tx of the proposed CSK-CDMA VLC system using red as an example.

Using the de-spread process in Rx, Color1 and Color2 can be recovered as they are transmitted in orthogonal code basis. Then, the magnitude of Spread-signal1 and Spread-signal2 are added to get the total red signal, which is modified to the level 0–255 by adding

the offset +120. In a process to adjust the 8-bit data depth (0–255). Finally, the output of Tx is [220, 100, 140, 20].

As shown in Figure 20. the received signal is de-spread after separating the red color from received RGB signal in the Rx. For User1, an offset of 120 is subtracted from the received signal before de-spreading it by Spreading code1. By dividing the inner product of [100, 20, 20, 100] and [1, -1, 1, -1] by the length of the spreading code (4), we get 60. Hence User1 and User2 can use the same technique to retrieve the green magnitude and the blue magnitude of Color1. Since the Rx can retrieve Color1 from RGB color domains, Table 5 can be used to de-map the two data bits emitted from the Tx.

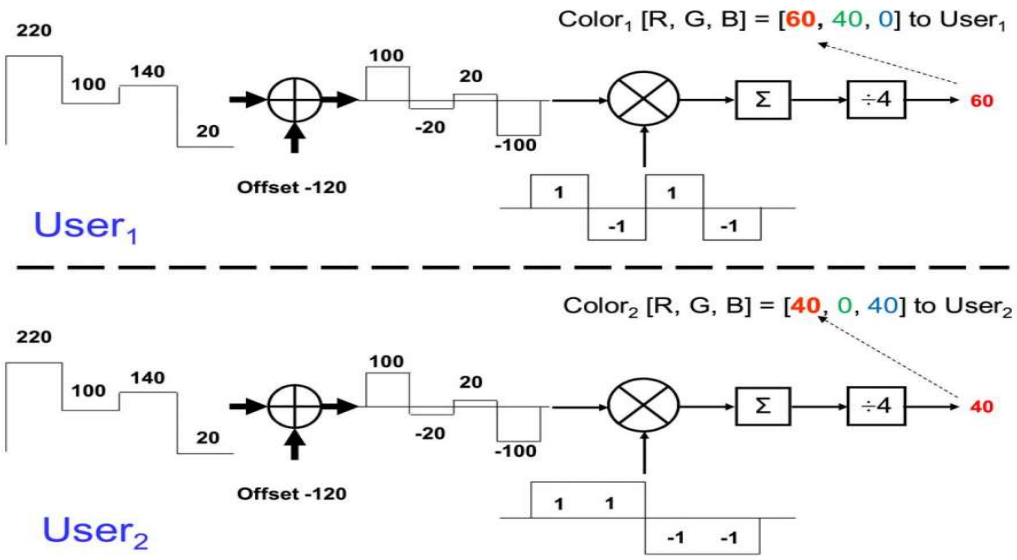

Figure 20. Rx of the proposed CSK-CDMA VLC system using red as an example.

CHAPTER 6

CONCLUSION

In this thesis, we have presented the key concepts, underlying principles and practical applications of visible light communications. In particular, we have studied the power distribution pattern and signal to noise ratio for line-of-sight indoor and vehicular applications. Several methods were used and studied to modify the SNR and power distribution levels. It is shown that in the absence of obstruction, the optical footprint is nearly circular and offers a platform for large- scale deployment in commercial environments, similar to micro and Pico cells.

In chapter 3, a differential optical receiver was used to reduce ambient light and other unwanted signals, thereby strengthening the desired optical signal. It is also shown that by changing the semi angle at half power, a minimum power of -2.3dBm and maximum power of 4.4 dBm for room model can be achieved. These measures also deliver a highly satisfactory SNR output as required by any optical communication system.

Chapter 4 provides a VLC model that only consider the outer dimensions of the SUV cabin. It has been illustrated that the rear passengers in vehicular model can, from the linearly scalable 1W LED source, achieve 7mW of received power. This is more than 100 times better than the typical IR LED.

This thesis emphasizes that VLC is a promising way of communication. There are numerous approaches that can be used in real time applications which will renovate the present and future living styles. This is shown in the proposed layout of the LED array to improve the optical power distribution.

The simulation results prove that after optimization of the half angle, the optical power distribution magnitude is larger and almost uniform. This optical footprint is nearly circular and can be used as a platform to develop micro and Pico cellular networks for commercial applications. Suggested applications would be in shopping malls, tunnels and subways, mines etc.

Furthermore, in chapter 5, RGB technology leads to the concept of CSK modulation. It is shown that CSK modulation, along with CDMA, can be used to implement the CSK-CDMA scheme, to develop optical CDMA networks. It should be noted that the RGB scheme is essentially a tri-cellular cluster, which is well known in cellular communication. Therefore, we envision that the proposed concept can be applied to develop optical CDMA network to offer high speed data communication.

In the future the analysis of hybrid channel, LOS and Non-LOS channels should be considered to accommodate multipath optical waveforms. Since it is nearly impossible to accommodate multipath components, we can develop an empirical model from collected data. Likewise, an empirical model can also be developed for intra vehicular applications. The presence of the passengers and the interior SUV structure should be considered to develop the empirical model.

Color planning is an idea that can be implemented using the RGB LEDs technology for indoor micro and Pico cellular color reuse schemes. This is similar to frequency planning used in cellular communications. One can look at combining these various techniques to increase the performance of VLC. These novel features, along with bit error rate calculations as well as handover procedures, need to be considered for future research.

APPENDICES

Appendix A

Calculating Optical power distribution in received optical plane for a FWHM of 35°or70° and the SNR of receiver with optimization MATLAB™ Code

```
%**********************************
% Thesis Code
% Rana Shaaban
% University of North Dakota
% December 2017
% Optical power distribution in received optical plane for
a FWHM of 35°or 70°
% The SNR of receiver with optimization
%**********************************
clc
clear all
close all

theta = 35;% 70°
% semi-angle at half power
ml=-log10(2)/log10(cosd(theta));
%Lambertian order of emission
P_LED=20;
%transmitted optical power by individual LED
nLED=60;
% number of LED array nLED*nLED
P_total=nLED*nLED*P_LED;
%Total transmitted power
Adet=1e-4;%1e-4
%detector physical area of a PD
Ts=1;
%gain of an optical filter
FOV=60;
%FOV of a receiver
 G_Con=6;
%gain of an optical concentrator
%%
lx=5; ly=5; lz=3;
% room dimension in meter
h=2.15;
%the distance between source and receiver plane
 [XT,YT]=meshgrid([lx/4 lx/4],[ly/4 ly/4]);
% position of LED
Nx=lx*5; Ny=ly*5;
% number of grid in the receiver plane
x=linspace(-lx/2,lx/2,Nx);
y=linspace(-ly/2,ly/2,Ny);
[XR,YR]=meshgrid(x,y);
D1=sqrt((XR-XT(1,1)).^2+(YR-YT(1,1)).^2+h^2);
% distance vector from source 1
cosphi_A1=h./D1;
```

```
% angle vector
receiver_angle=acosd(cosphi_A1);
H_A1=(ml+1)*Adet.*cosphi_A1.^(ml+1)./(2*pi.*D1.^2);
% channel DC gain for source 1
P_rec_A1=P_total.*H_A1.*Ts.*G_Con;
% received power from source 1;
P_rec_A1(find(abs(receiver_angle)>FOV))=0;
% if the anlge of arrival is greater than FOV, no current
isgenerated at the photodiode.
P_rec_A2=fliplr(P_rec_A1);
% received power from source 2, due to symmetry no need
separate calculations
P_rec_A3=flipud(P_rec_A1);
P_rec_A4=fliplr(P_rec_A3);
P_rec_total=P_rec_A1+P_rec_A2+P_rec_A3+P_rec_A4;
P_rec_dBm=10*log10(P_rec_total);
% SNR calculation
r=0.4;
q=1.602e-19;
Bn=0.562.^2*(10e6);
iam=5e-9;
Ba=50e6;
No=10e-22;
snr=(P_rec_total.^2.*(r.^2))./((2.*(P_rec_total).*q.*r.*Bn)
+(iam.^2.*Ba));
snr_db=10*log10(snr);
figure
surfc(x,y,snr_db);
xlabel('lenght of room 5 m')
ylabel('width of room 5 m')
zlabel('dB')
title('SNR')
figure
surfc(x,y,P_rec_dBm);
xlabel('lenght of room 6 m')
ylabel('width of room 5 m')
zlabel('dBm')
title('Optical Power Distribution')
figure
surfc(x,y,P_rec_total);
xlabel('lenght of room 6 m')
ylabel('width of room 5 m')
zlabel('mW')
title('Optical Power Distribution')
```

Appendix B

Calculating Optimized received power in mW for the rear and front passenger seats and the SNR of receiver for the rear and front passenger seats MATLAB™ Code

```
%**********************************
% Thesis Code
% Rana Shaaban
% University of North Dakota
% December 2017
% Optimized received power in mW for the rear and front
passenger seats
% The SNR of reciever for the rear and front passenger
seats
%**********************************
clc
clear all
close all


theta = 35;
% semi-angle at half power
ml=-log10(2)/log10(cosd(theta));
%Lambertian order of emission
P_LED=20;
%transmitted optical power by individual LED
nLED=50;
% number of LED array nLED*nLED
P_total=nLED*nLED*P_LED;
%Total transmitted power
Adet=1e-4;
%detector physical area of a PD
Ts=1;
%gain of an optical filter
FOV=60;
%FOV of a receiver
 G_Con=6;
%gain of an optical concentrator

lx=3.5; ly=1.6; lz=1.5;
% SUV dimension in meter
h=1;
%the distance between source and receiver plane
 XT=0; YT=0;
 % position of LED;

Nx=lx*5; Ny=ly*5;
% number of grid in the receiver plane
x=linspace(-lx/2,lx/2,Nx);
y=linspace(-ly/2,ly/2,Ny);
[XR,YR]=meshgrid(x,y);
```

```
D1=sqrt((XR-XT(1,1)).^2+(YR-YT(1,1)).^2+h^2);
% distance vector from source 1
cosphi_A1=h./D1;
% angle vector
receiver_angle=acosd(cosphi_A1);
H_A1=(ml+1)*Adet.*cosphi_A1.^(ml+1)./(2*pi.*D1.^2);
% channel DC gain for source
P_rec_A1=P_total.*H_A1.*Ts.*G_Con;
% received power from source ;
P_rec_A1(find(abs(receiver_angle)>FOV))=0;
% if the anlge of arrival is greater than FOV, no current
is generated at the photodiode.
P_rec_total=P_rec_A1;
P_rec_dBm=10*log10(P_rec_total);
% SNR calculation
r=0.4;
q=1.602e-19;
Bn=0.562.^2*(10e6);
iam=5e-9;
Ba=50e6;
No=10e-22;
snr=(P_rec_total.^2.*(r.^2))./((2.*(P_rec_total).*q.*r.*Bn)
+(iam.^2.*Ba));
snr_db=10*log10(snr);
figure
surfc(x,y,snr_db);
xlabel('lenght of SUV 3.5 m')
ylabel('width of SUV 1.6 m')
zlabel('dB')
title('SNR')
figure
surfc(x,y,P_rec_dBm);
xlabel('lenght of room 6 m')
ylabel('width of room 5 m')
zlabel('dBm')
title('Optical Power Distribution')
figure
surfc(x,y,P_rec_total);
xlabel('lenght of SUV 3.5 m')
ylabel('width of SUV 1.6 m')
zlabel('mW')
title('Optical Power Distribution')
colorbar
```

REFERENCES

[1] P. Pirinen, "A Brief Overview of 5G Research Activities," *Proc. 1st Int. Conf. 5G Ubiquitous Connect.*, pp. 17–22, 2014.

[2] D. A. Basnayaka and H. Haas, "Hybrid RF and VLC systems: Improving user data rate performance of VLC systems," in *IEEE Vehicular Technology Conference*, 2015, vol. 2015.

[3] M. Halper, "Here's what will really make LED office lighting take off | Lux Magazine | Luxreview.com | Americas | Home page," *Lux*, 2015. [Online]. Available: http://luxreview.com/article/2015/07/here-s-what-will-really-make-led-office-lighting-take-off.

[4] D. O'Brien *et al.*, "Indoor Visible Light Communications: challenges and prospects," *Free. Laser Commun. VIII*, vol. 7091, no. 0, pp. 1–9, 2008.

[5] A. Al-Fuqaha, M. Guizani, M. Mohammadi, M. Aledhari, and M. Ayyash, "Internet of Things: A Survey on Enabling Technologies, Protocols, and Applications," *IEEE Commun. Surv. Tutorials*, vol. 17, no. 4, pp. 2347–2376, 2015.

[6] J. R. Brodrick, "Energy Savings Potential of Solid-State Lighting in General Illumination Applications 2010 to 2030," *Energy*, no. February, pp. 1–54, 2010.

[7] P. H. Pathak, X. Feng, P. Hu, and P. Mohapatra, "Visible Light Communication, Networking, and Sensing: A Survey, Potential and Challenges," *IEEE Communications Surveys and Tutorials*, vol. 17, no. 4. pp. 2047–2077, 2015.

[8] L. Penubaku and K. Lakshmishree, “A survey on different techniques used for visible light communication,” in *2015 International Conference on Applied and Theoretical Computing and Communication Technology (iCATccT). IEEE, 2015.*, 2015, pp. 783–786.

[9] S.-B. Ryu, J.-H. Choi, J. Bok, H. Lee, and H.-G. Ryu, “High Power Efficiency and Low Nonlinear Distortion for Wireless Visible Light Communication,” *2011 4th IFIP Int. Conf. New Technol. Mobil. Secur.*, pp. 1–5, 2011.

[10] D. Ding, X. Ke, and L. Xu, “An optimal lights layout scheme for visible-light communication system,” in *2007 8th International Conference on Electronic Measurement and Instruments, ICEMI*, 2007, pp. 2189–2194.

[11] S. Rajagopal, R. D. Roberts, and S. K. Lim, “IEEE 802.15.7 visible light communication: Modulation schemes and dimming support,” *IEEE Commun. Mag.*, vol. 50, no. 3, pp. 72–82, 2012.

[12] K. B. Hunter, J. M. Conrad, and A. R. Willis, “Visible light communication using a digital camera and an LED flashlight,” in *IEEE SOUTHEASTCON 2014*, 2014, pp. 1–5.

[13] S. J. Lee and S. Y. Jung, “A SNR analysis of the visible light channel environment for visible light communication,” in *APCC 2012 - 18th Asia-Pacific Conference on Communications: “Green and Smart Communications for IT Innovation,”* 2012, pp. 709–712.

[14] W. H. Cai and T. T. Sun, “CTS: The new generation intelligent transportation

system," in *Proceedings - 2011 2nd International Conference on Innovations in Bio-Inspired Computing and Applications, IBICA 2011*, 2011, pp. 137–140.

[15] S. Verma, a Shandilya, and a Singh, "A model for reducing the effect of ambient light source in VLC system," *Adv. Comput. Conf. (IACC), 2014 IEEE Int.*, pp. 186–188, 2014.

[16] S. H. Chen and C. W. Chow, "Color-Shift Keying and Code-Division Multiple-Access Transmission for RGB-LED Visible Light Communications Using Mobile Phone Camera," *IEEE Photonics J.*, vol. 6, no. 6, 2014.

[17] J. M. Kahn, "Wireless infrared communications," *Proc. IEEE*, vol. 85, no. 2, pp. 265–298, 1997.

[18] F. R. Gfeller and U. Bapst, "Wireless In-House Data Communication via Diffuse Infrared Radiation," *Proc. IEEE*, vol. 67, no. 11, pp. 1474–1486, 1979.

[19] L. Grobe and A. Paraskevopoulos, "High-speed visible light communication systems," *Commun. ...*, no. December, pp. 60–66, 2013.

[20] J. M. Kahn, W. J. Krause, and J. B. Carruthers, "Experimental characterization of non-directed indoor infrared channels," *IEEE Trans. Commun.*, vol. 43, no. 2–4 pt 3, pp. 1613–1623, 1995.

[21] K. Cui, G. Chen, Q. He, and Z. Xu, "Indoor optical wireless communication by ultraviolet and visible light," *Proc. SPIE*, vol. 7464, p. 74640D–74640D–9, 2009.

[22] J. R. Barry, J. M. Kahn, W. J. Krause, E. A. Lee, and D. G. Messerschmitt,

"Simulation of Multipath Impulse Response for Indoor Wireless Optical Channels," *IEEE J. Sel. Areas Commun.*, vol. 11, no. 3, pp. 367–379, 1993.

[23] K. Lee, H. Park, and J. R. Barry, "Indoor channel characteristics for visible light communications," *IEEE Commun. Lett.*, vol. 15, no. 2, pp. 217–219, 2011.

[24] J. Grubor, S. Randel, K. D. Langer, and J. W. Walewski, "Broadband information broadcasting using LED-based interior lighting," *J. Light. Technol.*, vol. 26, no. 24, pp. 3883–3892, 2008.

[25] D. C. O'Brien, L. Zeng, H. Le-Minh, G. Faulkner, J. W. Walewski, and S. Randel, "Visible Light Communications: Challenges and possibilities," in *IEEE International Symposium on Personal, Indoor and Mobile Radio Communications, PIMRC*, 2008.

[26] P. Technologies, "Diffuse Reflectance – Theory and Applications," *Pike Technologies*, p. 2, 2011.

[27] T. Komine, J. H. Lee, S. Haruyama, and M. Nakagawa, "Adaptive equalization system for visible light wireless communication utilizing multiple white led lighting equipment," *IEEE Trans. Wirel. Commun.*, vol. 8, no. 6, pp. 2892–2900, 2009.

[28] S. Bourennane, M. Wolf, Z. Ghassemlooy, S. Long, and M. A. Khalighi, "Investigating channel frequency selectivity in indoor visible-light communication systems," *IET Optoelectron.*, vol. 10, no. 3, pp. 80–88, 2016.

[29] a. J. C. Moreira, R. T. Valadas, and a. M. de Oliveira Duarte, "Performance of

infrared transmission systems under ambient light interference," *IEE Proc. - Optoelectron.*, vol. 143, no. 6, p. 339, 1996.

[30] A. C. Boucouvalas, "Indoor ambient light noise and its effect on wireless optical links," *Optoelectron. IEE Proceedings-*, vol. 143, no. 6, pp. 334–338, 1996.

[31] H. Lu, Z. Su, and B. Yuan, "SNR and Optical Power Distribution in an Indoor Visible Light Communication System," pp. 1063–1067, 2014.

[32] S. - Faruque, S. - Faruque, and W. - Semke, "- Orthogonal on–off keying for free-space laser communications with ambient light cancellation," - *Opt. Eng.*, vol. 52, no. 9, p. 096113, 2017.

[33] S. Pergoloni, M. Biagi, S. Colonnese, R. Cusani, and G. Scarano, "Optimized LEDs Footprinting for Indoor Visible Light Communication Networks," *IEEE Photonics Technol. Lett.*, vol. 28, no. 4, pp. 532–535, 2016.

[34] R. J. Green and S. Member, "Optical Wireless with Application in Automotives," in *ICTON*, pp. 1–4, 2010.

[35] K. Dar, M. Bakhouya, J. Gaber, M. Wack, and P. Lorenz, "Wireless communication technologies for ITS applications [Topics in Automotive Networking]," *IEEE Commun. Mag.*, vol. 48, no. May, pp. 156–162, 2010.

[36] F. Bai and B. Krishnamachari, "Exploiting the wisdom of the crowd: Localized, distributed information-centric VANETs," *IEEE Commun. Mag.*, vol. 48, no. 5, pp. 138–146, 2010.

[37] M. D. Higgins, R. J. Green, and M. S. Leeson, “Optical wireless for intravehicle communications: A channel viability analysis,” *IEEE Trans. Veh. Technol.*, vol. 61, no. 1, pp. 123–129, 2012.

[38] IEEE Computer Society, “IEEE Standard for Local and metropolitan area networks - Part 15.7: Short-Range Wireless Optical Communication Using Visible Light,” *IEEE Std 802.15.7-2011*, vol. 1, no. September, pp. 1–286, 2011.

[39] R. J. Drost and B. M. Sadler, “Constellation design for color-shift keying using billiards algorithms,” in *2010 IEEE Globecom Workshops, GC’10*, pp. 980–984, 2010.

[40] T. C. W. Schenk, L. Feri, H. Yang, and J. P. M. G. Linnartz, “Optical wireless CDMA employing solid state lighting LEDs,” in *LEOS Summer Topical Meeting*, pp. 23–24, 2009.